

Provided for non-commercial research and education use.  
Not for reproduction, distribution or commercial use.



This article appeared in a journal published by Elsevier. The attached copy is furnished to the author for internal non-commercial research and education use, including for instruction at the authors institution and sharing with colleagues.

Other uses, including reproduction and distribution, or selling or licensing copies, or posting to personal, institutional or third party websites are prohibited.

In most cases authors are permitted to post their version of the article (e.g. in Word or Tex form) to their personal website or institutional repository. Authors requiring further information regarding Elsevier's archiving and manuscript policies are encouraged to visit:

<http://www.elsevier.com/copyright>



Contents lists available at ScienceDirect

## Journal of Colloid and Interface Science

www.elsevier.com/locate/jcis



# Interaction of sodium N-lauroylsarcosinate with N-alkylpyridinium chloride surfactants: Spontaneous formation of pH-responsive, stable vesicles in aqueous mixtures

Sampad Ghosh, Joykrishna Dey\*

Department of Chemistry, Indian Institute of Technology, Kharagpur 721 302, India

## ARTICLE INFO

## Article history:

Received 14 December 2010

Accepted 21 February 2011

Available online 1 March 2011

## Keywords:

Mixed surfactant

Synergism

Vesicles

Fluorescence

Microscopy

Light scattering

## ABSTRACT

The interaction of sodium N-lauroylsarcosinate (SLS) with N-cetylpyridinium chloride (CPC) and N-dodecylpyridinium chloride (DPC) was investigated in aqueous mixtures. A strong interaction between the anionic and cationic surfactants was observed. The interaction parameter,  $\beta$  was determined for a wide composition range and was found to be negative. The mixed systems were found to have much lower critical micelle concentration (*cmc*) and surface tension at *cmc*. The surfactant mixtures exhibit synergism in the range of molar fractions investigated. The self-assembly formation in the mixtures of different compositions and total concentrations were studied using a number of techniques, including surface tension, fluorescence spectroscopy, dynamic light scattering (DLS), transmission electron microscopy (TEM), confocal fluorescence microscopy (CFM). Thermodynamically stable unilamellar vesicles were observed to form upon mixing of the anionic and cationic surfactants in a wide range of composition and concentrations in buffered aqueous media. TEM as well as DLS measurements were performed to obtain shape and size of the vesicular structures, respectively. These unilamellar vesicles are stable for periods as long as 3 months and appear to be the equilibrium form of aggregation. Effect of pH, and temperature on the stability was investigated. The vesicular structures were observed to be stable at pH as low as 2.0 and at biological temperature (37 °C). In presence of 10 mol% of cholesterol the mixed surfactant vesicles exhibited leakage of the encapsulated calcein dye, showing potential application in pH-triggered drug release.

© 2011 Elsevier Inc. All rights reserved.

## 1. Introduction

In liposome-mediated delivery of therapeutic molecules, it is required to design responsive liposomes (or vesicles) capable of changing their properties in a controlled way under external stimuli, such as pH, salt concentration, temperature, and light. Consequently, pH-sensitive [1], thermo-responsive [2], and UV light sensitive [3] vesicles have been reported in the literature. This requires either integration of responsive functionality near the polar head-group of the bilayer-forming amphiphile or incorporation of an amphiphilic molecule which bears the responsive functionality. The rationale for designing pH-sensitive vesicles is to exploit the acidic environment of tumors to trigger release of entrapped guest/drug molecules through destabilization of bilayer membranes. Different classes of pH-sensitive liposomes have been proposed in the literature [1]. One class of liposomes uses combination of unsaturated phosphatidylethanolamines, such as dioleoyl-phosphatidylethanolamine (DOPE) and a mildly acidic amphiphile, such as oleic acid (OA). Although OA-containing liposomes are more

sensitive to pH, releasing their content below pH 6.5, they have been shown to be unstable in the presence of mouse and human plasma due to either extraction of OA from the membrane by albumin or through transfer to other membranes. This led to the use of other pH-sensitive amphiphiles, such as N-palmitoylhomocysteine, cholesterylhemisuccinate, diacylsuccinylglycerol, and N-(succinyl)dioleoylphosphatidyl-ethanolamine. The second class of liposomes is composed of lipid derivatives, which contains chemical bonds that can undergo acid-induced hydrolysis. A third class of liposomes utilizes pH-sensitive peptides. The most current class of liposomes, however, uses pH-sensitive polymers [4]. The latter three classes of liposomes also have unique advantages and disadvantages that may vary in importance depending on the desired application.

The use of non-ionic surfactant vesicles in drug delivery as an alternative to liposomes is now widely investigated. Recently, some pH-sensitive non-phospholipid formulations were reported in the literature [5]. Non-phospholipid vesicles based on the mixture of two oppositely charged single-chain surfactants are well known in the literature. After Kaler et al. reported the spontaneous formation of thermodynamically stable vesicles in dilute aqueous solution of single-tailed cationic and anionic surfactant mixtures [6], there have been numerous studies in the following years

\* Corresponding author. Fax: +91 3222 255303.

E-mail address: joydey@chem.iitkgp.ernet.in (J. Dey).

[7,8]. The stability of such vesicles is a result of nonideal mixing between the surfactants [9]. These cationic/anionic vesicles possess distinct microenvironments for the encapsulation of small guest molecules. In fact, this new method for stable vesicle formation has received considerable attention because of practical applications, such as templating nanoparticles [10], preparation of hollow spheres [11], encapsulation of probe molecules [12] and pharmaceutical drugs [13]. Recently, DNA compaction and encapsulation studies, envisioning gene delivery applications [14] have been carried out. There have been reports in the recent literature that mixtures of sodium salts of fatty acids and alkyltrimethylammonium halides form unilamellar vesicles in water [15].

In this work, we studied interaction of sodium N-lauroylsarcosinate (SLS), an anionic surfactant with two N-alkylpyridinium chloride (cationic) surfactants, N-dodecylpyridinium chloride (DPC) and N-cetylpyridinium chloride (CPC) in aqueous mixtures. SLS is a micelle-forming carboxylate surfactant and is widely used as a detergent. The cationic surfactants, DPC and CPC with a single alkyl chain also form small spherical micelles in the absence of salts or other additives. However, aqueous mixtures of SLS and CPC (or DPC) at a composition close to 1:1 were found to produce small unilamellar vesicles [16]. Therefore, we have investigated the detailed phase behavior of the mixed surfactant systems in a wide range of compositions. The aim of this work is to prepare non-phospholipid pH-sensitive vesicles from mixtures of the two oppositely charged surfactants. Here SLS has been used as a pH-sensitive molecule. Studies have shown that carboxylate surfactants including sodium salt of fatty acids and N-acyl amino acids have apparent  $pK_a$  values, typically in the range of 5.0–7.0, when dissolved in micelles of other surfactants [17]. Therefore they can be used as a pH-sensitive surfactant and thus micelle or membrane structure can be destabilized when the external pH is changed, usually from a neutral or slightly alkaline pH to an acidic pH. The microstructures formed by the SLS–CPC and SLS–DPC mixtures under different conditions have been characterized by a number of techniques, including surface tension, fluorescence probe, dynamic light scattering, and microscopy. The chain asymmetry affects on spontaneous vesicle formation has been examined. The effects of pH and temperature on vesicle stability were also studied. The mixed surfactant vesicles were also demonstrated to exhibit pH-induced leakage of the encapsulated calcein dye.

## 2. Experimental section

### 2.1. Materials

Sodium N-lauroylsarcosinate was obtained from Fluka. The cationic surfactants, CPC, DPC were procured from SRL, Mumbai, India. The fluorescent probes, 1,6-diphenyl-1,3,5-hexatriene (DPH), 5(6)-carboxyfluorescein (CF), and calcein (Aldrich) were recrystallized either from ethanol or acetone–ethanol mixture at least three times. Purity of all the probes was confirmed by the measurement of fluorescence emission as well as excitation spectra. All the reagents and solvents, e.g. ethanol, methanol, and acetone were of good quality commercially available and were purified and distilled fresh whenever required. Analytical grade potassium chloride, sodium dihydrogen phosphate, and sodium hydroxide were purchased from SRL, Mumbai, India. High quality Mili-Q (18.2 M $\Omega$ ) water was used for solution preparation.

### 2.2. Physical methods

#### 2.2.1. General instrumentation

$^1\text{H}$  NMR spectra were recorded on a Bruker SEM 200 instrument using TMS (trimethyl silane) as standard. UV–visible spectra were

recorded on a Shimadzu (model 1601) spectrophotometer. Thermo Orion model 710A + digital pH meter (EC India Ltd., Kolkata) using a glass electrode calibrated with a pH = 7.0 buffer was used to measure the pH of the solutions. All the measurements were carried out at room temperature (30 °C) unless otherwise mentioned. Temperature controlled measurements were carried out by use of a Thermo-Neslab RTE-7 circulating bath.

#### 2.2.2. Solution preparation

Samples were prepared by combining the cationic and anionic surfactants at a desired concentration and mixing ratio from the individual surfactant stock solution. After sealing the samples were mixed by simple hand agitation. The composition of the mixtures thus obtained is expressed in terms of molar fraction,  $X_1$  ( $=[\text{SLS}]/([\text{SLS}] + [\text{CPC}])$ ) of SLS. The pH of the samples was varied using 20 mM phosphate buffer having equal ionic strength. Since DPH is insoluble in water, a 1.0 mM stock solution of the probe in 20% (v/v) methanol–water mixture was prepared. The final concentration of the probe was adjusted to 5  $\mu\text{M}$  by addition of an appropriate amount of the stock solution. Prior to observation and measurements, the solutions were allowed to equilibrate at room temperature for a few hours.

#### 2.2.3. Surface tension measurements

The critical micelle concentration ( $cmc$ ) was determined by the surface tension (ST),  $\gamma$ , measurements performed by an automated Surface Tensiometer (Model 3S, GBX, France) using Du Nuöy ring detachment method. The temperature was maintained at  $30 \pm 0.1$  °C by constantly circulating thermostated water bath. The platinum–iridium ring was carefully cleaned with 50% ethanol–HCl solution and finally with distilled water. The instrument was calibrated and checked by measuring the  $\gamma$  of distilled water. For the determination of  $cmc$ , stock solutions of surfactants were made in Mili-Q (18.2 M $\Omega$ ) water. Progressive addition of the stock surfactant solution of known concentration was transferred using a Hamilton microsyringe to a Teflon beaker (properly cleaned with sulfochromic acid) containing known volume of water. The solution was gently stirred magnetically and allowed to equilibrate for  $\sim 5$  min at 30 °C and then  $\gamma$  was measured. Each measurement was repeated at least three times to obtain coherent  $\gamma$  value. The measured surface tension values were plotted as a function of the logarithm of total surfactant concentration ( $\log C$ ).

#### 2.2.4. Viscosity measurements

Viscosity of aqueous mixed surfactant solutions were measured by using a Vibro Viscometer (Model: SV-1A, A&D, Tokyo, Japan) instrument. The temperature of the solution was controlled by a Thermo-Neslab RTE-7 circulating water bath with a temperature accuracy of  $\pm 0.1$  °C. The solution was equilibrated for 5 min to get a constant viscosity value. All measurements were carried out at 30 °C. Reproducibility (triplicate) was checked for the samples and no significant differences ( $\pm SD$ ) were observed.

#### 2.2.5. Steady-state fluorescence measurements

Steady-state fluorescence anisotropy of DPH was measured on a Perkin Elmer LS-55 luminescence spectrometer equipped with filter polarizers that uses the L-format configuration. A quartz cell of 1-cm path length was used for all fluorescence measurements. For fluorescence anisotropy measurements in the presence of surfactant, DPH were excited at 350 nm and the fluorescence intensity was measured at 450 nm. A 430 nm cutoff filter was placed in the emission beam to eliminate the effects of scattered light, if any. The excitation and emission slit widths were 2.5 and 7.5 nm, respectively. The software supplied by the manufacturer automatically determined the correction factor and anisotropy value. In all the cases, the anisotropy values were averaged over an integration

time of 10 s and maximum number of five measurements for each sample. The temperature ( $30 \pm 0.1$  °C) of the water-jacketed cell holder was controlled by use of a Julabo F12 circulating bath.

### 2.2.6. Dynamic light scattering

The DLS measurements were carried out using Zetasizer Nano ZS (Malvern Instrument Lab, Malvern, UK) equipped with 4-mW He-Ne laser ( $\lambda_0 = 633$  nm) at a scattering angle  $173^\circ$ . The samples were filtered into the cell using 450 nm Millipore filter. The experiments were performed at  $\sim 30$  °C. The data for DLS were analyzed by second order cumulant fit [18].

### 2.2.7. Transmission electron microscopy

The morphological structures were observed with a JEOL-JEM 2100, Japan transmission electron microscope operating at an accelerating voltage of 200 kV at room temperature. A carbon coated copper grid was dipped in a drop of the aqueous surfactant solution for 1 min, excess solution was drained off with filter paper, air dried for an hour, and then negatively stained with freshly prepared 1% aqueous uranyl acetate. The specimens were kept in desiccators until before use.

### 2.2.8. Confocal fluorescence microscopy

All confocal fluorescence microscopy (CFM) imaging experiments were performed with a FV 1000 Olympus Confocal Microscope equipped with a laser scanning module (LSM) microscope and a PLAPON 60 $\times$  oil immersion objectives. The numerical aperture (NA) of LSM was 1.42. For CF-labeled vesicles, we used 488 nm laser and a 520 nm filter. For encapsulation of dyes into the vesicles the surfactant mixture and dye solution of desired concentration in methanol were gently mixed and then dried by rotary evaporation in a round bottom flask. The thin film of surfactant mixtures thus produced was soaked in water overnight and then appropriate volume of buffer was added to obtain clear solution. The excess dye was removed by dialysis for 10–12 h in a biodialyzer using an ultrafiltration cellulose acetate membrane (pore size 1000 Da MWCO, diameter 16 mm). An aliquot of the undiluted vesicle solution was pipetted into the microscope glass slides (Riviera, 25.4  $\times$  76.2 mm) and sealed with a cover slip and left to sit cover slip down for few minutes before analysis. All vesicles were imaged at room temperature and image projections of both cationic and anionic rich dye-trapped vesicles were analyzed using FV10-ASW 1.6 Viewer software.

## 3. Results and discussion

### 3.1. Solution behavior and surface activity

#### 3.1.1. Aqueous solubility

The phase behavior of the SLS–DPC and SLS–CPC mixtures at different mixing ratios and concentration was first investigated. It was observed that binary mixtures of SLS and CPC produced isotropic optically clear solutions at all compositions and total concentrations. However, the binary mixtures of SLS and CPC produced isotropic clear solutions only at  $X_1 \leq 0.40$  and at  $X_1 > 0.67$ . The dilute ( $< 2$  mM) mixtures of SLS and CPC with  $0.40 \leq X_1 \leq 0.67$  appeared turbid, which upon increase of total surfactant concentration and subsequent centrifugation resulted in two immiscible liquid phases, a oily layer on the top and the aqueous solution at the bottom. Similar behavior has been reported for many cationic/anionic mixed systems [19]. The oily phase is usually called as “coacervate” which is a 1:1 complex of the surfactants. In fact the  $^1\text{H}$  NMR spectrum (see Fig. S1 of “Supporting information”) of the oily phase obtained from the 1:1 mixture of SLS and CPC confirmed this.

#### 3.1.2. Surface tension

The surface tension ( $\gamma$ ) measurements were performed to determine *cmc* of the mixed surfactant systems. The breakpoint of the plots of  $\gamma$  vs.  $\log C$  for the aqueous mixed surfactant solution gives the *cmc*. The ST plots have been shown in Figs. S2 and S3 of “Supporting information”. The *cmc* values of pure SLS ( $C_1$ ), and CPC or DPC ( $C_2$ ) were reported [20] and are 14.57 mM, 0.9 mM, 16.2 mM, respectively. The *cmc* and other surface chemical properties were determined or approximately calculated from the curve for different compositions and are listed in Table 1. The *cmc* values of the both surfactant mixtures showed a drastic decrease than that of pure surfactant. Similar behavior was also observed with the  $\gamma_{\text{cmc}}$  values in different compositions. The *cmc* value increases slightly as the molar fraction ( $X_1$ ) of SLS increases or decreases as shown in Fig. 1. Similar synergism can also be found with the  $\gamma_{\text{cmc}}$

**Table 1**

Critical micelle concentration (*cmc*),  $\gamma_{\text{cmc}}$ ,  $\text{pC}_{20}$  and  $\beta$  parameter values of various compositions of SLS–CPC and SLS–DPC mixtures at 30 °C.

$X_1$	Properties			
	<i>cmc</i> ( $\pm 0.12$ ) (mM)	$\gamma_{\text{cmc}}$ (mN/m)	$\text{pC}_{20}$	$\beta$ ( $\pm 0.33$ )
<b>SLS–CPC</b>				
0.00	0.900 <sup>a</sup>	43.8	3.29	–
0.17	0.096	27.7	5.26	–14.48
0.20	0.073	27.2	5.42	–15.48
0.25	0.058	27.1	5.17	–16.26
0.33	0.037	27.0	5.21	–17.93
0.50	0.030	26.9	5.31	–18.76
0.67	0.039	27.0	5.23	–18.21
0.75	0.063	27.1	5.03	–16.59
0.80	0.084	27.3	4.94	–15.80
0.83	0.100	27.7	4.89	–15.38
1.00	14.57 <sup>a</sup>	33.8	2.35	–
<b>SLS–DPC</b>				
0.00	16.20 <sup>a</sup>	47.7	1.94	–
0.17	0.612	26.0	4.27	–13.86
0.20	0.509	25.9	4.32	–14.38
0.25	0.486	25.8	4.40	–14.29
0.33	0.442	25.7	4.47	–14.38
0.50	0.391	25.5	4.52	–14.64
0.67	0.463	25.7	4.48	–14.17
0.75	0.510	25.9	4.35	–14.07
0.80	0.600	26.0	4.23	–13.68
0.83	0.655	26.1	4.17	–13.53
1.00	14.57	33.8	2.35	–

<sup>a</sup> Taken from Ref. [20].

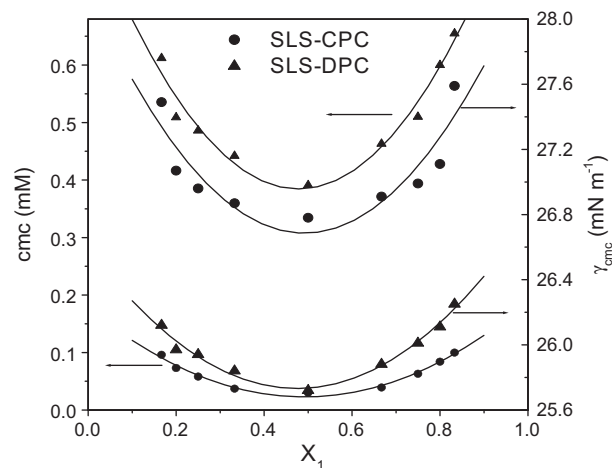


**Fig. 1.** Plots of *cmc* and  $\gamma_{\text{cmc}}$  vs. molar fraction ( $X_1$ ) of SLS of (●) SLS–CPC, (▲) SLS–DPC mixtures at 30 °C.

value (Fig. 1). Such a large decrease of *cmc* of SLS can be explained by the formation of vesicles along with mixed micelles containing 1:1 ion-pair complex and CPC surfactant. The ion-pair complex may be considered as a double chain surfactant. Thus strong anionic-cationic synergism among hydrocarbon chains of the constituent surfactants results in a lower *cmc* value. The increase of *cmc* with the increase or decrease of molar fraction is due to the increased electrostatic repulsion between surfactant headgroups as a consequence of gradual incorporation of more surfactants in the mixed micelle.

A small quantity of SLS or CPC (or DPC) was enough to significantly lower the limiting surface tension (the relatively constant value reached after the *cmc*) and the surface tension values for any given total surfactant concentration. It was also enough to significantly increase the *cmc*. Further increases in SLS or CPC content continued this trend, however, with increasingly less significance.

The mixed surfactant systems have very good surface activity compared to pure surfactant as indicated by the respective  $\gamma_{cmc}$  and detergency number,  $pC_{20}$  (negative logarithm of surfactant concentration at which the surface tension of water is reduced by 20 units). The  $pC_{20}$  values of all the surfactant mixtures are greater than 4.0, which suggest that they are good surface-active agents [21]. The data in Table 1 indicate that the surface activity is highest when the surfactants are present in equimolar quantities ( $X_1 = 0.50$ ). In addition, *cmc* and  $\gamma_{cmc}$  of the mixed systems attains minimum value at equimolarity. For all the surfactant mixtures, the tendency of surface adsorption is higher as compared to micelle formation in the bulk water, which means that these mixtures can be used as good detergent.

### 3.1.3. Surfactant-surfactant interactions

The  $\beta$  parameter obtained from regular solution theory [22] has been shown to be useful in understanding the nature of interactions between two surfactants in solution. Usually the interaction parameter,  $\beta$  is determined by measuring *cmc* of the corresponding surfactant mixtures. The interaction between SLS and CPC or SLS and DPC surfactants in the mixed aggregate was measured by calculating  $\beta$  from equations derived using Rubingh's theory [23]. According to regular solution theory [22,24] the *cmc*'s of surfactant mixtures are given by

$$C = X_{1m} \cdot f_1 \cdot C_1 = X_1 \cdot C_{12} \quad (1)$$

where  $C_{12}$  and  $C_1$  are the *cmc*'s of the mixture and component 1 (SLS), respectively,  $C$  and  $X_1$  are the concentration and molar fraction of surfactant 1 (SLS) in solution, respectively,  $X_{1m}$  is the mole fraction of surfactant 1 in the mixed micelle, and  $f_1$  is the activity coefficient, which is given by the equation

$$\ln f_1 = \beta(1 - X_{1m})^2 \quad (2)$$

It should be noted that  $\beta$  is a dimensionless interaction parameter that can be experimentally determined from the *cmc* values according to the equation [22,24]

$$\beta = \frac{\ln(C_{12}X_1/C_1X_{1m})}{(1 - X_{1m})^2} \quad (3)$$

Since  $f_1 = [C_{12}(1 - X_1)/C_2(1 - X_{1m})]$ , Eq. (2) can be rewritten as

$$\frac{X_{1m}^2 \ln(C_{12}X_1/C_1X_{1m})}{(1 - X_{1m})^2 \ln\{C_{12}(1 - X_1)/C_2(1 - X_{1m})\}} \quad (4)$$

where  $C_2$  is the *cmc* of surfactant 2 (CPC or DPC).

From the *cmc* values,  $\beta$  value was calculated using Eqs. (3) and (4). The interaction parameter  $\beta$  thus obtained for different molar fraction ( $X_1$ ) of SLS have been listed in Table 1. From the data in Table 1, it can be found that the  $\beta$  values for all compositions of binary mixtures are negative, which suggests that the interaction

between SLS and CPC (or DPC) surfactants is more attractive in the mixed micelle than the self-interaction of the surfactants before mixing. According to the regular solution theory the  $\beta$  parameter should be independent of composition [25,26]. However, in the present mixed surfactant system, it is observed that the  $\beta$  value gradually becomes less negative as the  $X_1$  value deviates from 0.50. The interaction is strongest in equimolar mixture ( $X_1 = 0.50$ ). The synergistic interaction is further supported by the fact that the  $|\beta|$  value is greater than  $|\ln(C_1/C_2)|$ . Similar behavior has also been reported for other systems [27]. Also it is interesting to observe that compared to the SLS-DPC system the  $\beta$ -value is more negative in the case of SLS-CPC system for a given composition, suggesting stronger interaction in the latter mixture. However, it has been reported that  $\beta$ -values only explain the interaction between headgroups of the two surfactants, it does not include the interaction between hydrocarbon chains of the surfactants when the chain lengths are different [27]. Accordingly, one would expect similar  $\beta$ -values for both systems for a given composition as the headgroups are same. This implies that interaction between hydrocarbon chains also contribute to the value of  $\beta$  parameter.

## 3.2. Self-assembly formation

### 3.2.1. Fluorescence probe studies

Considering the rich aggregation behaviors and the challenging characterization in mixed cationic and anionic surfactant systems, the transition between micelles and vesicles in these systems was studied systematically. In the present work, mixed cationic and anionic surfactant systems, SLS-CPC and SLS-DPC at different composition and different concentration, were selected to study the transition. It is known that the molecular arrangement will become more closely and orderly packed in the mixed surfactant aggregates [28]. Consequently, the polarity of the hydrophobic region will decrease when the aggregate transforms from micelles to vesicles or reverse.

Depolarization degree of fluorescence emission is an indication of the rotational diffusion of an excited fluorophore and is widely exploited to probe the microenvironment in the organized microstructure. To investigate the structural change that occurs at different concentration and composition above the *cmc* of the mixed surfactant system, steady-state fluorescence anisotropy ( $r$ ) measurements were performed using DPH as fluorescent probe. DPH is a well-known membrane fluidity probe and has been used for studying many lipid bilayer membranes [29]. Fig. 2 shows the variation of  $r$ -value of DPH probe with the molar fraction ( $X_1$ ) of SLS for SLS-CPC (0.5 mM) and SLS-DPC (2 mM) mixtures. For both mixed systems under study, the  $r$ -value increases with the increase of SLS content up to  $X_1 = 0.50$ , indicating decrease of microfluidity of the mixed aggregates. Further increase of SLS content, however, decreased the  $r$ -value. The higher value of  $r$  suggests an ordered environment around the DPH probe in the self-assemblies compared to that of micellar aggregates. This means existence of bilayer aggregates in the surfactant mixtures over a wide range of composition. The possibility of formation of rod-like micelles could be ruled out based on the solution viscosity ( $\eta$ ) data. Normally formation of rod-like micelles results in a large increase of solution viscosity. Therefore, we measured  $\eta$ -values for both types of mixtures (2 mM) at different molar fraction of SLS. The data have been presented in the inset of Fig. 2. As seen for both type of mixtures, the  $\eta$ -value initially increases with the increase of  $X_1$  and then decreased passing through a maximum at  $X_1 = 0.50$ . This is exactly similar to the variation of fluorescence anisotropy of DPH. However, the highest value of  $\eta$  observed for SLS-CPC mixture is less than 1.3 mPa s, which is very low and cannot be attributed to formation of rod-like micelles.

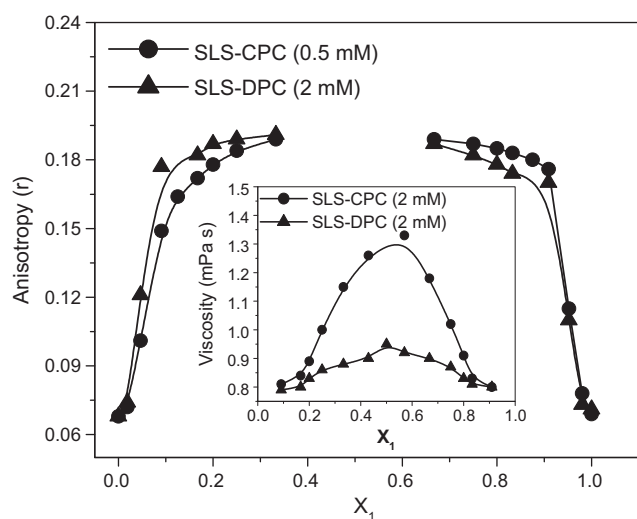


**Fig. 2.** Variation of fluorescence anisotropy ( $r$ ) of DPH probe with molar fraction,  $X_1$  of SLS in SLS-CPC (0.5 mM) and SLS-DPC (2 mM) systems; inset: plot of solution viscosity ( $\eta$ ) vs. molar fraction ( $X_1$ ) of SLS in 2 mM SLS-CPC and SLS-DPC mixtures.

Based on the results presented in Fig. 2, we chose an anionic-rich composition (4:1) and a cationic-rich composition (1:4) for further studies as described below. The  $r$ -value of DPH was measured in 1:4 and 4:1 mixtures of both SLS-DPC and SLS-CPC systems at different concentration. The data are presented in Fig. 3. It can be observed that  $r$ -value is relatively high for both compositions of the mixed systems and gradually increases with the total concentration above  $cmc$  reaching maximum at ca. 5 mM. The  $r$ -value remains unchanged until 20 mM for SLS-CPC system and 40 mM for SLS-DPC system. However, above this limiting concentration the  $r$ -value starts to fall with further increase of concentration in both the mixed systems. The results indicate that the bilayer aggregates exist over a large concentration range. The decrease of  $r$ -value at a much higher concentration can be attributed to transformation of bilayer structures to either spherical micelles or rod-like aggregates. This was confirmed by the results of viscosity measurements.

As mentioned earlier, the formation of rod-like aggregates is normally evidenced by the increase of solution viscosity,  $\eta$ . In con-

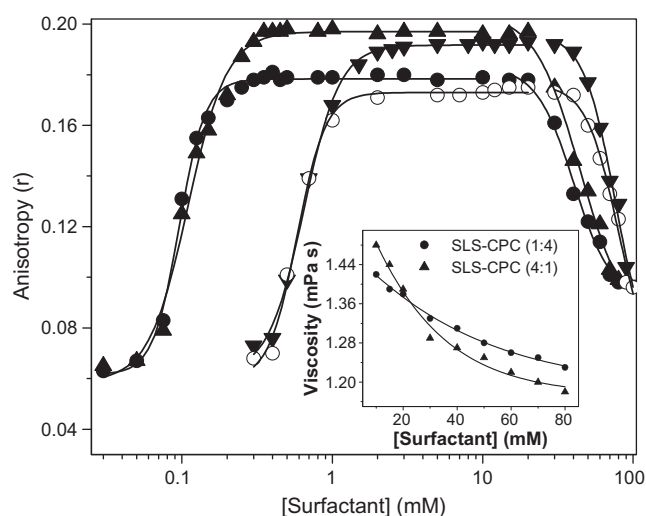


**Fig. 3.** Variation of anisotropy ( $r$ ) of DPH with [surfactant]: (●) SLS-CPC (1:4), (▲) SLS-CPC (4:1), (▼) SLS-DPC (1:4), (○) SLS-DPC (4:1); Inset: Plot of solution viscosity ( $\eta$ ) in SLS-CPC (1:4 and 4:1) mixtures as a function of [surfactant].

trast, for both the mixed systems the  $\eta$ -value was observed to be small and was found to decrease with the increase of total surfactant concentration. Representative plots of variation of  $\eta$  as a function of total surfactant concentration have been shown in the inset of Fig. 3. Relatively small viscosity value in dilute solution indicate existence of bilayer aggregates of spherical shape i.e. vesicles. Thus the decrease of  $r$ -value with concomitant decrease of viscosity suggests transition of vesicles-to-spherical micelles in mixtures with mol ratios 1:4 and 4:1.

### 3.2.2. Microscopy

Macroscopic phase behaviors are closely related to the microstructures in the aqueous solution. Therefore morphology of the aggregates was studied using TEM and CFM techniques. Representative TEM pictures of the 1:4 and 4:1 SLS-CPC mixtures have been shown in Fig. 4. A characteristic vesicular system containing large particles along with small particles is observed for both anionic and cationic-rich compositions. The slides of micrograph illustrate that the vesicles are almost spherical in shape and the diameters are ranging from 50 nm to 200 nm. Also the vesicles appear to be unilamellar in nature. Small unilamellar vesicles (SUVs) having similar sizes could also be observed in dilute 1:1 SLS-CPC mixtures in neutral pH (image C). It is interesting to note that vesicle structures that are formed in 1:4 mixtures are retained even in pH 2.0 solutions (image D). However, the size of the vesicles (ca. 25–50 nm) is reduced in acidic medium.

In support of the TEM results we have performed CFM measurements with the different mixtures. The CFM images as shown in Fig. S4 of “Supporting information” clearly exhibit spherical vesicles with dye (CF) filled aqueous core. The size of the vesicles formed in both 1:4 and 4:1 SLS-CPC mixtures is in the range 100–200 nm. On the other hand, the vesicle diameter in 1:4 and 4:1 SLS-DPC mixtures ranges between 100 and 500 nm. Relatively larger size of the vesicles as compared to corresponding TEM images may be due to higher concentration of the surfactant mixture used in the case of CFM measurements. Also in contrast to TEM, CFM only “see” the large objects. It should also be noted that TEM procedure involved drying of the sample, which could reduce the vesicle diameter.

### 3.2.3. Size distribution of vesicles

For direct measurement of the hydrodynamic diameter ( $d_H$ ) of the particles in solutions of the two mixed system we used DLS method. The histograms in Fig. 5 show size distributions of the aggregates in 1:4 and 4:1 mixtures of both systems in dilute solutions. A bimodal distribution can be observed for both compositions with both types of mixed systems, suggesting coexistence of two types of aggregates. The relatively larger aggregates (compared to micelle) having  $d_H$  around 3–10 nm can be attributed to disk-like mixed micelles. The large aggregates having  $d_H$  in the range 70–200 nm, on the other hand, must be due to bilayer vesicles which are produced from disk-like micelles. The size of the vesicles is thus closely similar with those observed in the TEM and CFM images. It is observed that in 4:1 mixtures, vesicle sizes are slightly smaller compared to that of 1:4 mixtures for both SLS-CPC and SLS-DPC systems. The DLS measurements clearly suggest that vesicle size does not change significantly with the increase of total surfactant concentration.

## 3.3. Stability of vesicles

### 3.3.1. Aging effect

Aging effect on the vesicles was investigated by measuring solution turbidity at different time intervals. The turbidity of the samples (20 mM) of both SLS-CPC and SLS-DPC mixed systems with surfactant composition 1:4 was measured at 450 nm and the re-

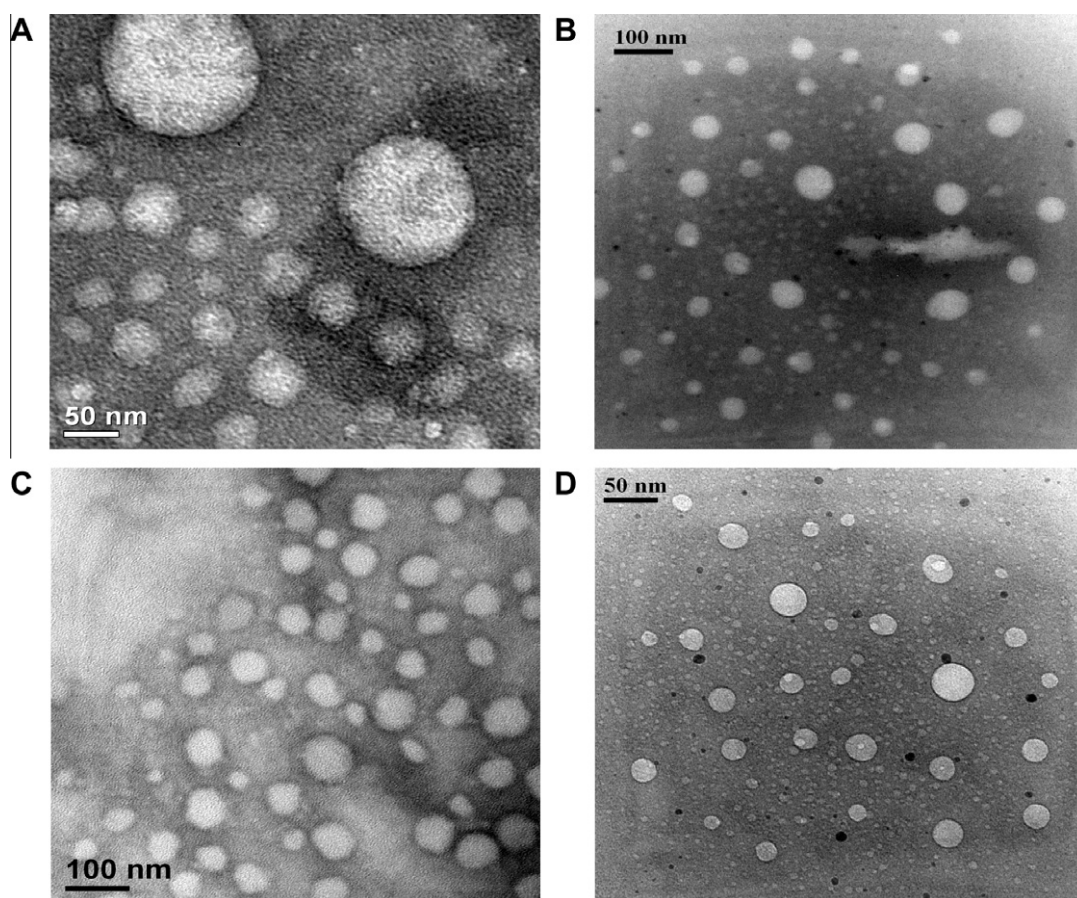


Fig. 4. Negatively stained TEM micrographs of (A) 1 mM (1:4), (B) 1 mM (1:1), (C) 1 mM (4:1), and (D) 1 mM (1:4; pH 2.0) SLS-CPC mixtures.

sults are illustrated in Fig. 6. Although the solutions looked isotropic, the turbidity appears because of the scattering of light by the vesicular aggregates. In fact, the extent of turbidity depends on the size and population of vesicles. The scattering result indicates that turbidity increases only slightly with time. The plots in Fig. 6 show that there is a small but sharp increase of turbidity of the samples in the initial aging interval of about 40 days and then remains at the equilibrium value for at least 100 days. The initial increase of the turbidity arises from the formation and growth of vesicles while the subsequent constant turbidity suggests high evolution stability with aging time. The plots in Fig. 6 also show that turbidity of SLS-DPC mixture is higher than that of SLS-CPC mixture, which means vesicle sizes are bigger in the case of former than in the latter mixture. This is consistent with the results of microscopic and DLS studies.

### 3.3.2. pH Effect

Since one of the surfactants in the mixtures has  $\text{COO}^-$  headgroup, the structure of the vesicles is expected to change with the variation of solution pH. The steady-state fluorescence anisotropy of DPH probe in the surfactant mixtures was found to decrease with the decrease of pH of the solution as shown by the plots in Fig. 7. It is found that for 1:4 and 4:1 mixtures of both SLS-CPC (0.5 mM) and SLS-DPC (2 mM) the  $r$ -value is highest at pH 9.0, and can be considered a better condition for vesicle formation in these mixed systems. It is observed that  $r$ -value decreases by a large extent in going from pH 9.0 to 2.0. The sigmoid change of the  $r$ -value indicates two-state process and can be attributed to protonation of the  $\text{COO}^-$  group, which reduces ionic attractions between the headgroups. This results in a decrease of ordering in the

headgroup region of the surfactants and thus affects the compact packing in the interior of the bilayer aggregates as manifested by the decrease of  $r$ -value with the decrease of pH. The inflection point of the plots in Fig. 7 can be taken as the  $\text{pK}_a$  of N-laurylsarcosine (NLS) in the mixed surfactant vesicles. The  $\text{pK}_a$  value thus obtained is ca. 5.0 in the mixed systems. Such titration could not be carried out with the 4:1 mixture of SLS-DPC system as precipitation occurs at  $\text{pH} < 4.0$ . However, absence of any precipitation in the case of 4:1 mixture of SLS-CPC system could be due to solubilization of the uncharged NLS molecules within the vesicle structure.

The data presented in Fig. 7 show that the  $r$ -value is relatively high even at a pH as low as 2.0 at which SLS is completely protonated. The presence of uncharged NLS molecules, however, reduces ionic repulsion between positively charged headgroups of DPC or CPC surfactants increasing hydrocarbon chain packing in comparison to pure DPC or CPC micelles. This is reflected by the relatively high  $r$ -value at low pH. This explains existence of vesicular structures along with micelles even at low pH. Indeed, the TEM micrograph (Fig. 4) of 1:4 SLS-CPC mixed systems (1 mM) at pH 2.0 revealed existences of spherical vesicles. The above observations suggest that even though stable vesicles are formed in both 1:4 and 4:1 mixtures of both systems at lower pH, the membrane rigidity decreases with the decrease of pH, which may cause leakage of entrapped pharmaceutical molecule (if any) within the aqueous core of the vesicles. This has been demonstrated below.

### 3.3.3. Temperature effect

It is well known that increase of temperature is effective in removing hydration water decreasing the hydration repulsion be-

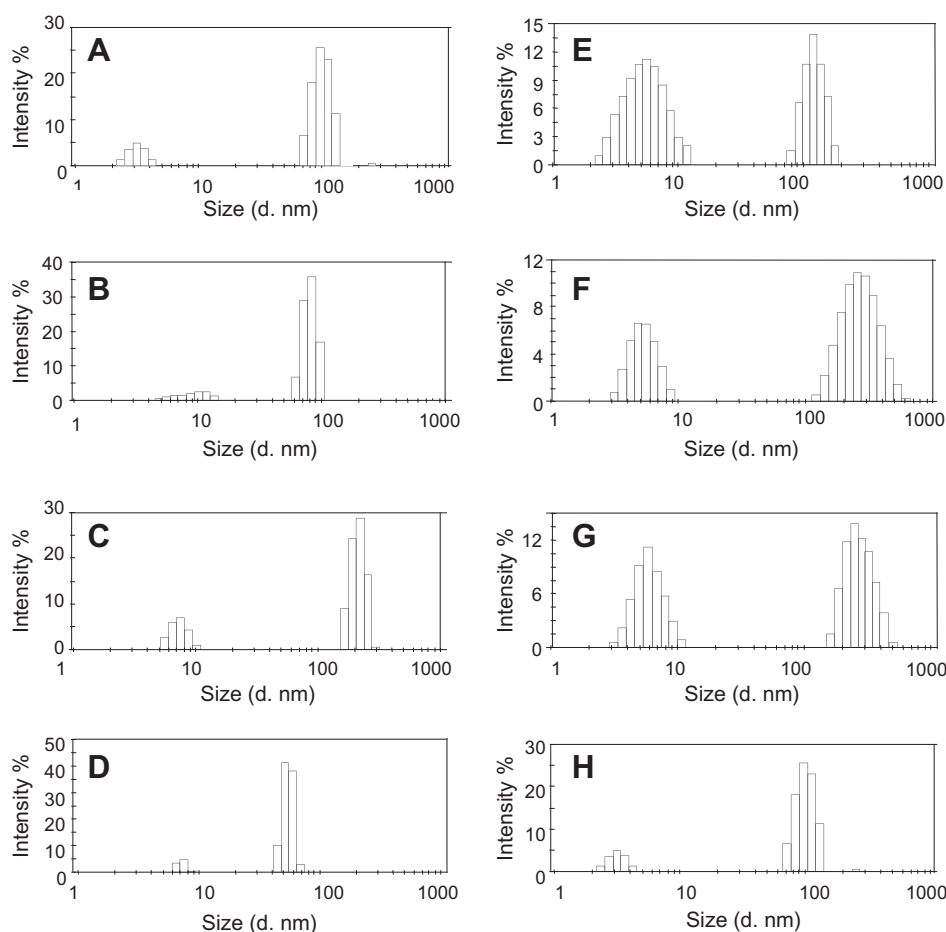


**Fig. 5.** Size distribution histograms of vesicles in (A) 1 mM SLS-CPC (1:4), (B) 20 mM SLS-CPC (1:4), (C) 50 mM SLS-CPC (1:4), (D) 1 mM SLS-CPC (4:1), (E) 2 mM SLS-DPC (1:4), (F) 50 mM SLS-DPC (1:4), (G) 90 mM SLS-DPC (1:4), and (H) 2 mM SLS-DPC (4:1).

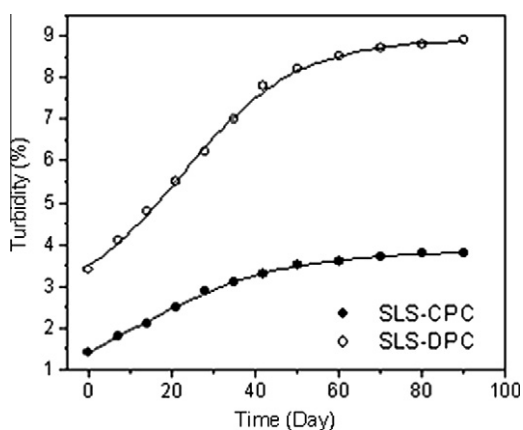


**Fig. 6.** Plot of turbidity ( $100 - \%T$  at 450 nm) of 1:4 SLS-CPC and SLS-DPC mixtures (20 mM) as a function of aging time.

tween colloid particles. When the hydration repulsion becomes very low such that the total interactions changed from repulsive to attractive, the aggregation of the colloid particles takes place. Although such effect is rarely observed in vesicle systems [30,31], several micellar systems [32] were found to exhibit temperature-induced aggregation. Vesicle aggregation induced by the increase of temperature, however, has been reported in the case of *n*-dodecyltributylammonium bromide/sodium *n*-dodecyl sulfate (SDS) mixed system [30].

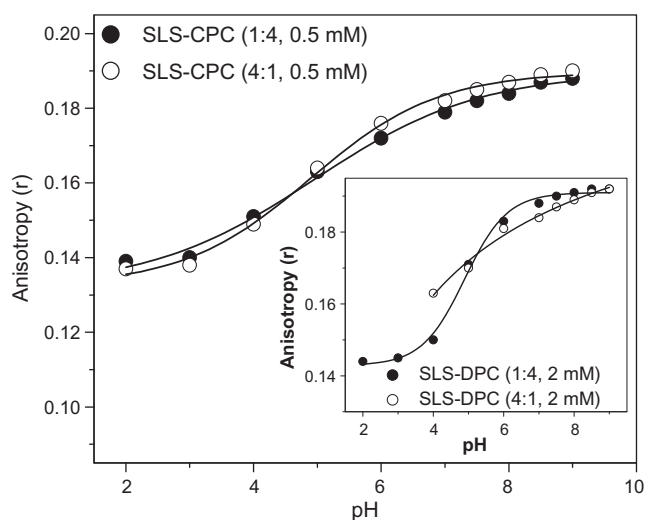


**Fig. 7.** Variation of fluorescence anisotropy ( $r$ ) of DPH as a function of pH (ionic strength = 0.108) in the presence of SLS-CPC and SLS-DPC (inset) mixtures of different composition at 30 °C.

In the present systems, the influence of temperature on vesicle aggregation was also investigated by monitoring fluorescence anisotropy of DPH probe. It was interesting to observe that the  $r$ -value of DPH in the presence of SLS-CPC or SLS-DPC mixtures decreases with the increase of temperature (Fig. 8). The large change

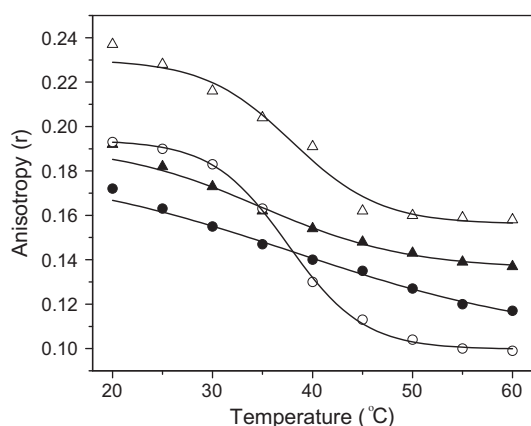


**Fig. 8.** Variation of fluorescence anisotropy ( $r$ ) of DPH as a function of temperature in the presence of (●) 1 mM 1:4 SLS-CPC, (▲) 10 mM 1:4 SLS-CPC, (○) 2 mM 1:4 SLS-DPC, and (△) 20 mM 1:4 SLS-DPC system.

in anisotropy with the rise in temperature can be associated with gel–fluid phase transition of vesicles, which is an important parameter that affects immunogenicity. Thus the temperature corresponding to the inflection point can be taken as the phase transition temperature,  $T_m$ . It is interesting to note that the  $T_m$  value is higher for dilute solution ( $38 \pm 0.2$  °C) in comparison to concentrated solution ( $37 \pm 0.3$  °C) of both types of surfactant mixtures.

### 3.4. Entrapment and release studies

The entrapment of CF dye in mixed surfactant vesicles has been shown earlier by CFM images (Fig. S4 of “Supporting information”). This demonstrates their ability to entrap water-soluble dye which implies that the vesicles are closed and contain an inner aqueous compartment. Similar experiments were also carried out with calcein, a pH-sensitive fluorescent dye whose fluorescence emission intensity decreases with the decrease of pH. The vesicles containing entrapped calcein were prepared in the presence of 10 mol% cholesterol (Chol) to enhance membrane rigidity. Fluorescence spectrum (Fig. 9) of entrapped calcein ( $\lambda_{ex} = 495$  nm and  $\lambda_{em} = 520$  nm) was measured immediately after dilution of the vesicle phase (of 1:4 SLS-CPC mixture) containing entrapped dye in buffered solution of desired pH. As expected the calcein fluorescence

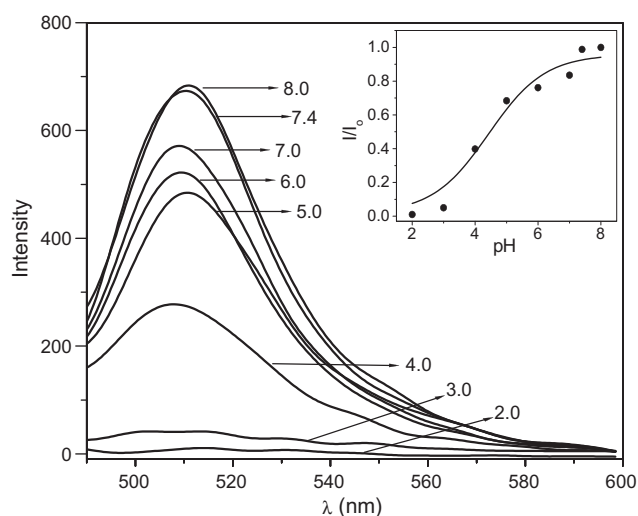


**Fig. 9.** Fluorescence spectrum of entrapped calcein in different pH (having equal ionic strength, 0.108 M) in presence of 20 mM SLS-CPC (1:4) containing 10 mol% Chol; inset: plot of relative fluorescence intensity ( $I/I_0$ ) as a function of pH at 30 °C.

is quenched when the pH of the bulk aqueous phase is reduced, indicating pH-triggered release of the dye. The plot of relative fluorescence intensity as a function of pH is also shown in the inset of Fig. 9. The pH corresponding to the inflection point of the sigmoid plot can be taken as the  $pK_a$  (ca. 5.0) of the NLS in the vesicles containing 10 mol% Chol. It is clear that almost 50% of the entrapped dye is released at pH around 5.0. Similar behavior was also observed in the case of 4:1 SLS-CPC mixture. The corresponding fluorescence spectra and titration curve have been depicted in Fig. S5 of “Supporting information”.

## 4. Conclusions

In summary, interaction between sodium N-lauroylsarcosinate (SLS) and N-cetylpyridinium chloride (CPC) or N-dodecylpyridinium chloride (DPC) in aqueous mixtures was investigated. It was found that the interaction parameter,  $\beta$  for all compositions of binary mixtures is negative, suggesting strong interaction between oppositely charged headgroups. In contrast to literature reports, the results, however, also suggested significant contribution of the hydrophobic interaction between hydrocarbon chains. The mixed systems were found to have much lower  $cmc$  and surface tension at  $cmc$  compared to the pure components. The surfactant mixtures exhibit synergism in the range of compositions investigated. Due to large synergism behavior of the mixed surfactant systems they exhibit novel solution and interfacial properties. Very low  $cmc$  of the mixed surfactant systems indicate probable use as a detergent with less-effect on the environment because of surfactant biodegradability and less amount in the environment.

Mixing of the anionic and cationic surfactants in a wide range of composition and concentrations in buffered aqueous media resulted in the formation of unilamellar vesicles having diameters in the range 100–200 nm. In contrast to literature reports, it has been shown that chain length asymmetry is not required for spontaneous vesicle formation in the present cationic/anionic mixed systems. However, it was observed that chain length asymmetry caused tighter packing of the hydrocarbon chains in membrane bilayer. These unilamellar vesicles were found to be stable at room temperature for periods as long as 3 months and appear to be the equilibrium form of aggregation. We have shown that the stability of such mixture of solutions can be tuned by variation of pH. The vesicular structures were observed to be stable in pH as low as 2.0 (in the case of SLS-CPC system) and at temperatures above 37 °C. It has been demonstrated that the mixed surfactant vesicles can entrap water-soluble molecules. However, the mixed vesicles containing 10 mol% cholesterol exhibits burst release of encapsulated calcein dye when pH of the bulk solution is reduced. Thus from the above studies it is concluded that the mixed surfactant vesicles can have potential application in the field of pH-triggered drug release. It is concluded that the mixed surfactant vesicles can be efficiently used as a drug delivery vehicle.

## Acknowledgments

Authors gratefully acknowledge Department of Science and Technology, New Delhi for financial support (Grant No. SR/S1/PC-18/2005) of this work. We are thankful to Dr. N. Sarkar and Mr. D. Gayen for assistance with the DLS and confocal microscopic measurements, respectively.

## Appendix A. Supplementary material

Supplementary data associated with this article can be found, in the online version, at [doi:10.1016/j.jcis.2011.02.054](https://doi.org/10.1016/j.jcis.2011.02.054).

## References

- [1] (a) D.C. Drummond, M. Zignani, J.-C. Leroux, *Prog. Lipid Res.* 39 (2000) 409–460;  
 (b) P. Venugopalan, S. Jain, S. Sankar, P. Singh, A. Rawat, S.P. Vyas, *Pharmazie* 57 (2002) 659–671;  
 (c) E. Fattal, P. Couvreur, C. Dubernet, *Adv. Drug Deliv. Rev.* 56 (2004) 931–936.
- [2] (a) M.H. Gaber, K. Hong, S.K. Huang, D. Papahadjopoulos, *Pharm. Res.* 12 (1995) 1407–1416;  
 (b) M.H. Gaber, N.Z. Wu, K. Hong, S.K. Huang, M.W. Dewhirst, D. Papahadjopoulos, *Int. J. Radiat. Oncol. Biol. Phys.* 36 (1996) 1177–1187.
- [3] C. Wang, Q. Chen, H. Xu, Z. Wang, X. Zhang, *Adv. Mater.* 22 (2010) 2553–2555.
- [4] (a) N. Sakaguchi, C. Kojima, A. Harada, K. Kono, *Bioconjugate Chem.* 19 (2008) 1040–1048;  
 (b) M. Zignani, D.C. Drummond, O. Meyer, K. Hong, J.-C. Leroux, *Biochim. Biophys. Acta* 1463 (2000) 383–394;  
 (c) N. Murthy, J.R. Robichaud, D. Tirrel, P.S. Stayton, A.S. Hoffman, *J. Controlled Release* 61 (1999) 137–143.
- [5] (a) M.F. Francis, G. Dhara, F.M. Winnik, J.-C. Leroux, *Biomacromolecules* 2 (2001) 741–749;  
 (b) M. Carafa, L.D. Marzio, C. Marianecchi, B. Cinque, G. Lucania, K. Kajiwara, M.G. Cifone, E. Santucci, *Eur. J. Pharm. Sci.* 28 (2006) 385–393;  
 (c) L.D. Marzio, C. Marianecchi, B. Cinque, M. Nazzari, A.M. Cimini, L. Cristinino, M.G. Cifone, F. Alhaique, M. Carafa, *Biochim. Biophys. Acta* 1778 (2008) 2749–2756.
- [6] E.W. Kaler, A.K. Murthy, B.E. Rodriguez, J.A.N. Zasadzinski, *Science* 245 (1989) 1371–1374.
- [7] (a) E. Marques, B.F. Silva, U. Olsson, *Langmuir* 24 (2008) 10746–10754;  
 (b) C.Z.T. Vautrin, M. Schneider, M. Tanaka, *J. Phys. Chem. B* 108 (2004) 7986–7991.
- [8] (a) N. Elkadi, F. Martins, D. Clause, P.C. Schulz, *Colloid Polym. Sci.* 281 (2003) 353–362;  
 (b) E. Marques, A. Khan, M.G.da. Miguel, B. Lindman, *J. Phys. Chem.* 97 (1993) 4729–4736;  
 (c) J. Hao, Z. Yuan, W. Liu, H. Hoffmann, *J. Phys. Chem. B* 108 (2004) 5105–5112.
- [9] S. Safran, P. Pincus, D. Andelman, *Science* 248 (1990) 354–356.
- [10] (a) J.H. Fendler, *Membrane Mimetic Approach to Advanced Materials*, Springer, Verlag, Berlin, 1992;  
 (b) W.L. Yu, J. Pei, W. Huang, G.X. Zhao, *Mater. Chem. Phys.* 49 (1997) 87–92;  
 (c) I.I. Yaacob, A.C. Nunes, A. Bose, *J. Colloid Interface Sci.* 171 (1995) 73–84.
- [11] (a) H.P. Hentze, S.R. Raghavan, C.A. McKelvey, E.W. Kaler, *Langmuir* 19 (2003) 1069–1074;  
 (b) C.A. McKelvey, E.W. Kaler, J.A. Zasadzinski, B. Coldren, H.T. Jung, *Langmuir* 16 (2000) 8285–8290;  
 (c) M. Kepczynski, J. Lewandowska, M. Romek, S. Zapotoczny, F. Ganachaud, M. Nowakowska, *Langmuir* 23 (2007) 7314–7320;  
 (d) S. Pevzner, O. Regev, A. Lind, M. Linden, *J. Am. Chem. Soc.* 125 (2003) 652–653.
- [12] (a) C. Caillet, M. Hebrant, C. Tondre, *Langmuir* 16 (2000) 9099–9102;  
 (b) A. Fischer, M. Hebrant, C. Tondre, *J. Colloid Interface Sci.* 248 (2002) 163–168.
- [13] E.J. Danoff, X. Wang, S.H. Tung, N.A. Sinkov, A.M. Kemme, S.R. Raghavan, D.S. English, *Langmuir* 23 (2007) 8965–8971.
- [14] (a) R.S. Dias, B. Lindman, M.G. Miguel, *J. Phys. Chem. B* 106 (2002) 12600–12607;  
 (b) M. Rosa, M.da.G. Miguel, B. Lindman, *J. Colloid Interface Sci.* 312 (2007) 87–97.
- [15] D. Kopetzki, Y. Michina, T. Gustavsson, D. Carriere, *Soft Matter* 5 (2009) 4212–4218.
- [16] M. Ambühl, F. Bangerter, P.L. Luisi, P. Skrabal, H.J. Watzke, *Langmuir* 9 (1993) 36–38.
- [17] C. Whiddon, C. Bunton, O. Soderman, *J. Phys. Chem. B* 107 (2003) 1001–1005.
- [18] R. Pecora (Ed.), *Dynamic Light Scattering: Applications of Photon Correlation Spectroscopy*, New York and London, 1985.
- [19] K.L. Stellner, J.C. Amante, J.F. Scamehorn, J.H. Harwell, *J. Colloid Interface Sci.* 123 (1988) 186–200.
- [20] (a) N.I. Venkataraman, V.V.R. Subrahmanyam, *J. Indian Chem. Soc.* 62 (1985) 507–512;  
 (b) B. Simoncic, J. Span, *Acta Chim. Slov.* 45 (1998) 143–152.
- [21] M.J. Rosen, *Surfactants and Interfacial Phenomena*, third ed., John Wiley and Sons, New York, 2004.
- [22] D.N. Rubingh, in: K.L. Mittal (Ed.), *Solution Chemistry of Surfactants*, vol. 1, Plenum Press, New York, 1979, pp. 337–354.
- [23] M.J. Rosen, *Surfactants and Interfacial Phenomena*, second ed., John-Wiley, New York, 1989.
- [24] M.J. Rosen, X.Y. Hua, *J. Colloid Interface Sci.* 86 (1982) 164–172.
- [25] (a) A.A. McLachlan, D.G. Marangoni, *J. Colloid Interface Sci.* 295 (2006) 243–248;  
 (b) F. Li, G.-Z. Li, J.-B. Chen, *Colloids Surf. A* 145 (1998) 167–174.
- [26] (a) A.M. Misselyn-Bauduin, A. Thibaut, J. Grandjean, G. Broze, R. Jerome, *Langmuir* 16 (2000) 4430–4435;  
 (b) D. López-Díaz, I. García-Mateos, M.M. Velázquez, *Colloids Surf. A* 270–271 (2005) 153–162;  
 (c) Z.-Y. Wang, S.-F. Zhang, Y. Fang, L.-Y. Qi, *J. Surfact. Deterg.* 13 (2010) 381–385.
- [27] (a) H. Maeda, *J. Colloid Interface Sci.* 172 (1995) 98–105;  
 (b) C.C. Ruiz, J. Aguiar, *J. Mol. Phys.* 97 (1999) 1095–1103.
- [28] (a) Z.J. Yu, G.X. Zhao, *J. Colloid Interface Sci.* 130 (1989) 421–431;  
 (b) J.B. Huang, G.X. Zhao, *Colloid Polym. Sci.* 274 (1996) 747–753.
- [29] (a) B.R. Lentz, *Chem. Phys. Lipids* 64 (1993) 99–116;  
 (b) J.R. Lakowicz, *Principles of Fluorescence Spectroscopy*, Plenum Press, New York, 1983, p. 132.
- [30] H.Q. Yin, J.B. Huang, Y.Q. Gao, H.L. Fu, *Langmuir* 21 (2005) 2656–2659.
- [31] H.Q. Yin, Y.Y. Lin, J.B. Huang, *Langmuir* 23 (2007) 4225–4230.
- [32] (a) S. Kumar, D. Sharma, Z.A. Khan, K.-ud-Din, *Langmuir* 17 (2001) 5813–5816;  
 (b) Z.-J. Yu, X. Zhang, G. Xu, G.-X. Zhao, *J. Phys. Chem.* 94 (1990) 3675–3681;  
 (c) G.G. Warr, T.N. Zemb, M. Drifford, *J. Phys. Chem.* 94 (1990) 3086–3092;  
 (d) S. Kumar, D. Sharma, Z.A. Khan, K.-ud-Din, *Langmuir* 18 (2002) 4205–4209.